Sustainable Energy & Fuels, Vol. 1, Issue 8, 2017, pp. 1788-1794
DOI:10.1039/C7SE00280G

# Table of Contents Entry

Acid catalyst promotes transmethylation in anisole decomposition through dual electrophilic attack mechanism, lowering intrinsic energy barriers by most 60 kcal/mol.

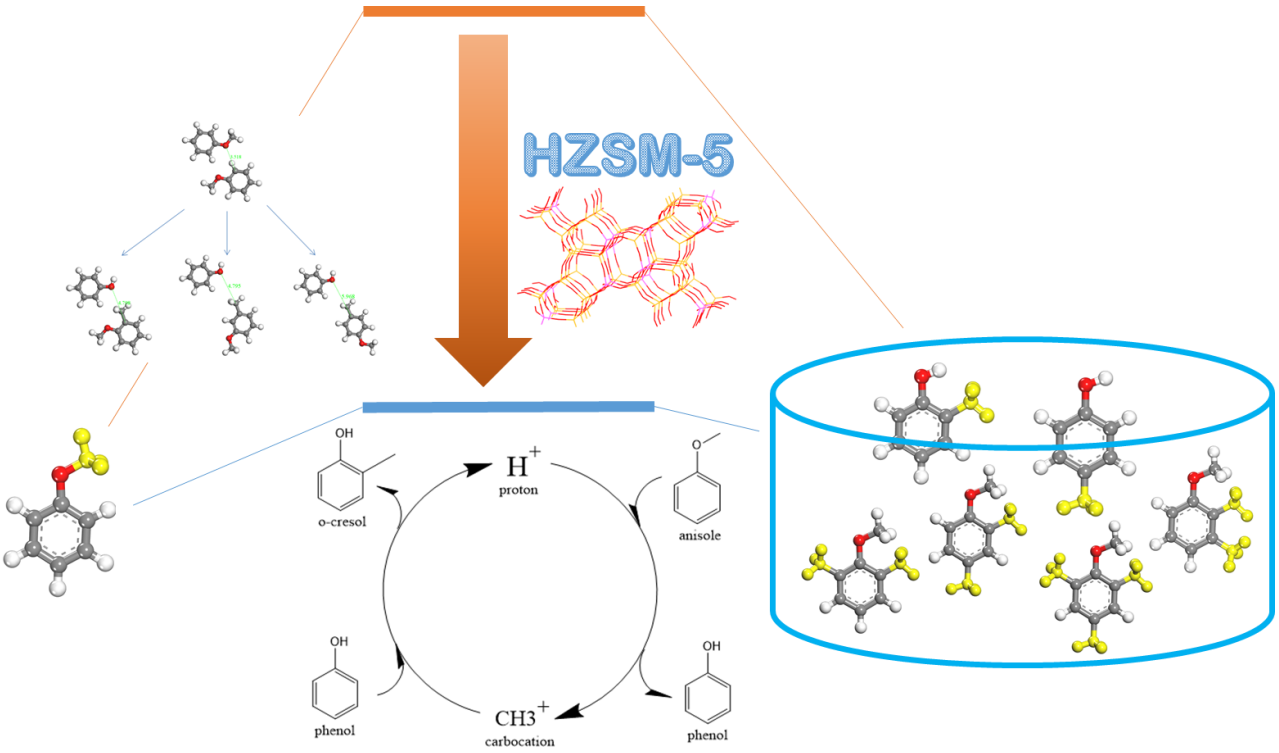


Published by Royal Society of Chemistry. This is the Author Accepted Manuscript issued with:
Creative Commons Attribution Non-Commercial License (CC:BY:NC 4.0).
The final published version (version of record) is available online at DOI:10.1039/C7SE00280G
Please refer to any applicable publisher terms of use.

# Mechanism of transmethylation in anisole decomposition over Brønsted acid sites: Density Functional Theory (DFT) study

Jiajun Zhang[ab], Beatriz Fidalgo[b], Athanasios Kolios[b], Dekui Shen[a*], Sai Gu[c]

* Corresponding author: Dekui Shen, Email: 101011398@seu.edu.cn

[a] Key Laboratory of Energy Thermal Conversion and Control of Ministry of Education, Southeast University, Nanjing, China

[b] School of Water, Energy and Environment, Cranfield University, Cranfield, United Kingdom

[c] Faculty of Engineering and Physical Sciences, University of Surrey, Surrey, United Kingdom

**Abstract:** In this work, the mechanism and intrinsic reaction energy barriers of transmethylation, as the initial stage of the catalytic and non-catalytic anisole decomposition, were investigated by Density Functional Theory (DFT). Molecule analyses indicated that methyl free radical transfer happened in the absence of catalyst, and the catalytic transmethylation over Brønsted acid sites was considered based on the dual electrophilic attack mechanism with protonation and carbocation substitution respectively. Reactions modelling for the formation of methyl-contained compounds in both non-catalytic and catalytic anisole decomposition indicated that the energy barriers were significantly decreased in the presence of catalyst by 60 kcal/mol at the most in the case of o-cresol. The results also revealed that the intrinsic transmethylation orientation preferred the ortho- and para-positions on the acceptor compounds contained oxygen-rich substituents due to its large electronegativity, and the lowest energy barrier was observed in the case of transmethylation towards the para-position of the cresol molecule (54.1 kcal/mol).

**Key words**: lignin; catalytic decomposition; model compound; modelling; phenolic compounds; substituent

## 1. Introduction

Lignin is an abundant aromatic-rich bio-resource; approximately 63 million tones are extracted annually mainly from the pulp and paper industry [1,2]. The fast pyrolysis of lignin has been investigated since the late 1970s, and is accepted as a feasible and viable route to convert

lignin into value added fuel additives [3–5]. However, the primary bio-oil produced from fast pyrolysis cannot be directly used in fuel applications. This is because of its inadequate properties, such as acidity, low calorific value, and low stability, which are a consequence of its high oxygen content in composition. The effective removal of the oxygen by catalytic upgrading is therefore crucial for making the bio-oil compatible with the existing fossil fuel infrastructure and for widening its use [6,7]. Catalytic cracking of bio-oil is one of the conversion routes usually suggested for deoxygenation, and zeolites with dispersed Brønsted acid sites, such as HZSM-5, have been proven as suitable catalysts for this process [8–11].

The methoxy group is an oxygen containing functional group which abundantly exists in components present in the bio-oil obtained from the fast pyrolysis of lignin, such as anisole, guaiacol, syringol and their derivatives [12]. Understanding the reactivity of the methoxy group is required to properly assess the complete catalytic upgrading process of these lignin-derived aromatic compounds. Anisole is often used as a model compound to investigate the reactivity of lignin-derived compounds containing the methoxy functional group, because this is the only functional group present in the molecule [13]. Transmethylation reaction has been observed to be the primary reaction taking place in anisole decomposition, leading to the prominent production of phenolic compounds [14–18].

Catalytic transmethylation over acid sites has been reported for phenol alkylation in the presence of methanol [19–23]. A few authors have described the transmethylation in the decomposition of anisole over acid sites consisting of isomerization, dealkylation, and intermolecular methyl transfer [24,25]. However, available literature mainly focused on the general study of pathways and kinetic parameters for the transmethylation reactions, with little details on catalysis mechanisms despite their importance to understand the entire catalytic process [26]. Although it is widely accepted that Brønsted acid sites play a dominant role in anisole decomposition [14,19,24], the precise mechanism for transmethylation over the acid sites is still controversial. Different, and sometimes hardly consistent, reaction pathways and mechanisms have been proposed for explaining the same chemical process in previous studies [19–23]. This might attributed to that transition state is key to understanding chemical reaction mechanism, but it is extremely unstable and hard to capture by means of experimental studies [27]. Wang et al. [16] have proposed hydrolysis as the first stage of the

anisole conversion, with little interaction of the acid sites, followed by the alkylation of phenol with methanol. Thilakaratne et al. [28] proposed the transmethylation mechanism based on the formation of a methenium ion during anisole decomposition on the Brønsted acid site. There has been other study suggesting the formation of a methyl carbocation directly by the methyl group in the anisole molecule [14,24,25,28,29], nevertheless, the studies have seldom addressed how the carbocation is formed and to what extent it affects the transmethylation reaction. In most previous studies, further evidence to prove the proposed mechanism regarding the transmethylation, or to evaluate the reactions based on the mechanism were not provided.

Despite experimental results being highly valuable to understand the overall reaction and products distribution at a macroscopic level, they present limitations in unravelling the reaction mechanism at molecular level. Density Functional Theory (DFT) modelling is based on the calculation of electrons interactions, and has been widely used as a systematic and convincing approach in explaining molecular properties and mechanisms for many reactions [30–34]. Compared to experimental approach, DFT calculation can provide intrinsic information of reactions regarding to detailed interaction between molecules and acid site, independently of the very short life span of the transition states, radicals and ions existing in the reactions. The microscale modelling of catalysis by DFT can also disregard complex impacts of macroscale factors (e.g. framework effects) and allows focusing on the reaction regarding its intrinsic properties. However, DFT calculation for transmethylation and related reactions has little been reported in the literature.

The aim of this work is to investigate by means of DFT modelling the mechanism of transmethylation as a primary reaction of the non-catalytic and catalytic decomposition of anisole, and to identify the effects of Brønsted acid sites on transmethylation. Compounds such as phenol, benzene, toluene, anisole, cresol, xylenol and tri-methyl phenol were investigated. The transfer orientation preference of the electrophilic substituents on relevant molecules was also studied. In addition, various possible reaction pathways of the transmethylation reaction were evaluated to address energy barriers during formation of major product compounds.

## 2. Computational method

The first-principles density functional theory plus dispersion (DFT-D) calculations were implemented in the DMol$^3$ module available in Materials Studio 2016 from BIOVIA [35,36]. The double numerical plus polarization (DNP) basis set was used to calculate the valence orbital of all the atoms, including a polarization p-function on all hydrogen atoms. The numerical basis sets in DMol$^3$ minimize or even eliminate basis set superposition error (BSSE), in contrast to Gaussian basis sets, in which BSSE can be a serious problem [37,38]. Calculations used the generalized gradient corrected approximation (GGA) [39] treated by the Perdew−Burke−Ernzerhof (PBE) exchange-correlation potential with long-range dispersion correction via Grimme's scheme [40]. The self-consistent field (SCF) procedure was used with a convergence threshold of $10^{-6}$ au on the energy and electron density. Geometry optimizations were performed with a convergence threshold of 0.002 Ha/Å on the gradient, 0.005 Å on displacements, and $10^{-5}$ Ha on the energy. The real-space global cut-off radius was set to 5 Å. In this study, no symmetry constraints were used for any cluster models. The transition state was completely determined by the LST/QST method, and confirmed by the unique imaginary frequency as shown in Table S1 in the supplementary information and Intrinsic reaction coordinate (IRC) calculation. Milliken charges were assigned to each bond to address the bond order, and Hirshfeld charges were assigned to each atom for the function selected as the Fukui field [41]. Radical Fukui analysis was applied to the phenol molecule to establish its reactivity to free radical attack in non-catalytic reactions. Electrophilic Fukui analysis was applied to anisole and phenol molecules to determine their reactivity to carbocation attack in catalytic reactions. The same computation condition was applied for both catalytic and non-catalytic modellings; in the case of catalytic reactions modelling, mainly Brønsted acid was considered. The initial configuration of the ZSM-5 catalysts was obtained from the siliceous ZSM-5 crystal, and an 8T model was used to simulate the performance of a Brønsted acid site [31,32]. The energy barrier for transmethylation reaction was determined by the difference between the transition state and reactant energies. The relative energy of the transition state and product was defined as the energy difference with the reactant respectively. All the energies were calculated at 0K to investigate the intrinsic reactions of transmethylation.

## 3. Results and discussions

### 3.1 Mechanism for transmethylation in anisole decomposition

The weakest bond in anisole molecule was observed for $C_{SP}^{3}$-O (as shown in Fig S2(a), Bond ID C8-O7), indicating that both the non-catalytic and catalytic thermal decomposition of anisole is preferably initiated at this site [29].

In the case of the non-catalytic decomposition of anisole, the molecule is subsequently cracked into free radicals, with a methyl radical being formed, which substitutes the hydrogen molecule on a phenol molecule to produce cresols [29], and the free radical substitutions are more likely to occur at the ortho-position and para-position of the phenol molecule (based on radical Fukui analysis (Fukui (0)) to phenol molecule, shown in Fig S3(a)). A previous experimental work by the group of J. Zhang et al [42] concluded the preferential formation of cresols at temperatures lower than 650°C during the non-catalytic decomposition of anisole. It should be noticed that due to there is no obvious intermediate compound existing in the non-catalytic transmethylation reactions, they are more likely to occur as one step reactions.

In the case of the catalytic decomposition of anisole over Brønsted acid sites, it has been largely recognized that the transmethylation reaction is induced by a proton that dissociates from the acid site and launches an electrophilic attack on the reactant [14,43–46]. The transmethylation mechanism is proposed to proceed through carbocation transfers in the case of catalytic decomposition of anisole, as shown in Fig 1.

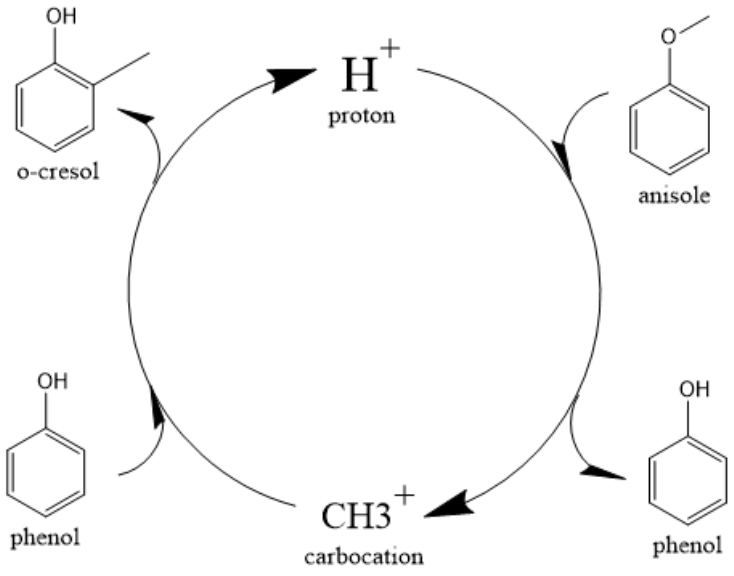

*Fig 1. Dual electrophilic attack mechanism of catalytic transmethylation*

The catalytic process of transmethylation can be divided into two steps. The first step consists of the methyl group cleavage in the anisole molecule; an initial electrophilic attack is launched by the proton dissociated from the catalyst acid site to the O atom (based on the electrophilic Fukui (Fukui (-)) analysis to anisole molecule, as shown in Fig S2(b)), and the methyl carbocation is released. A second electrophilic attack is launched by the methyl carbocation group; the group is likely to substitute the hydrogen atom at the o- and p-positions on the phenol ring (based on the electrophilic Fukui analysis (Fukui (-)) to phenol molecule, as shown in Fig S3(b)). The displaced free proton simultaneously interacts with the catalyst to recover the Brønsted acid site and maintain the catalytic activity throughout the reaction. Transition state compounds normally exist for a very short time due to instability; however, the methyl carbocation attached to the active site during the transmethylation process is a relatively stable structure with zero valent. Consequently, it can be considered as an intermediate compound, rather than a transition state compound, therefore it is possible to consider the methyl carbocation cleavage and the carbocation substitution reactions as separate steps in the catalytic transmethylation. The mechanism described in Fig 1 shows that the use of Brønsted acid catalyst replaces the one-step reaction of direct methyl free radical transfer observed for the non-catalytic reaction by a two-step process [25]. The mechanism also shows constant maintenance of acid sites in the catalyst by proton recovery throughout the reaction. Further reaction modelling was carried out considering the mechanism proposed here.

It is worth noting that in both non-catalytic and catalytic decomposition of anisole, the methyl group transfers not only to phenol but also to other compounds such as benzene, toluene, and even non-decomposed anisole present in the reaction media [42]. All the transmethylation processes are initiated from methyl cleavage.

### 3.2 Modelling of non-catalytic and catalytic transmethylation of anisole to phenol

The transmethylation reactions with a phenol molecule in the non-catalytic and catalytic decomposition of anisole were modelled. Both non-catalytic and catalytic transmethylation models were built by locating equidistantly the reactant molecules (about 3Å) to minimize any possible position-related errors. The catalytic transmethylation was modelled based on the

dual electrophilic attack mechanism proposed in Fig 1, considering the system containing methyl carbocation on the acid site as the intermediate compound (see Fig 2). The modelling was implemented in two stages: methyl carbocation cleavage from anisole over the catalyst active site, and transfer of the carbocation to the surrounding molecules. The transition states for both stages are denoted as TS1 and TS2 respectively. The non-catalytic transmethylation model was built according to the free radical mechanism, and the transition state of the reaction is denoted as TS. The cleavage energy of the carbocation from the anisole molecule (for TS1) and the energy barriers for the methyl carbocation transfer to ortho-, meta-, and para-positions of phenol (for TS2) during the catalytic transmethylation of anisole to form cresol via phenol, as predicted by the model, are shown in Fig 3. The transition state (TS) and corresponding energy barriers for the non-catalytic transmethylation of anisole to form n-cresol are shown for comparison.

As can be seen in Fig 3, the transmethylation to the ortho-position of phenol presented a lower energy barrier than the meta-position and para-position transfers both in non-catalytic and catalytic decomposition. This result indicates that ortho-position transmethylation is more likely to occur to the phenol molecule, which agrees with the experimental observations found elsewhere [42]. In short, experiments showed that o-cresol was formed at a lower temperature (550˚C) than p-cresol (600˚C) in non-catalytic anisole decomposition, and most multi-methyl phenolic compounds presented the ortho-position occupied by a methyl group in the catalytic anisole decomposition [42]. In addition, the model pointed to the highest energy barrier for the meta-position transfer. This is in agreement with experimental results, which exhibited no evidence of m-cresol formation [42]. However, it should be noted that the results in this study show the intrinsic properties of the reaction, and the experimental yields obtained are normally subjected to other effects, such as the framework topology effects of different zeolites. For example, shape selectivity of microporous zeolites plays a key role in the catalyst promoting the production of para-cresol [25].

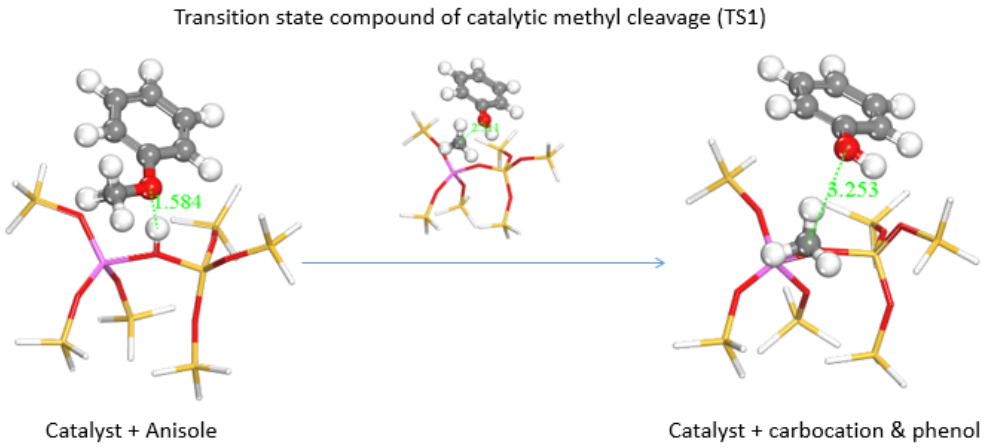


(a)

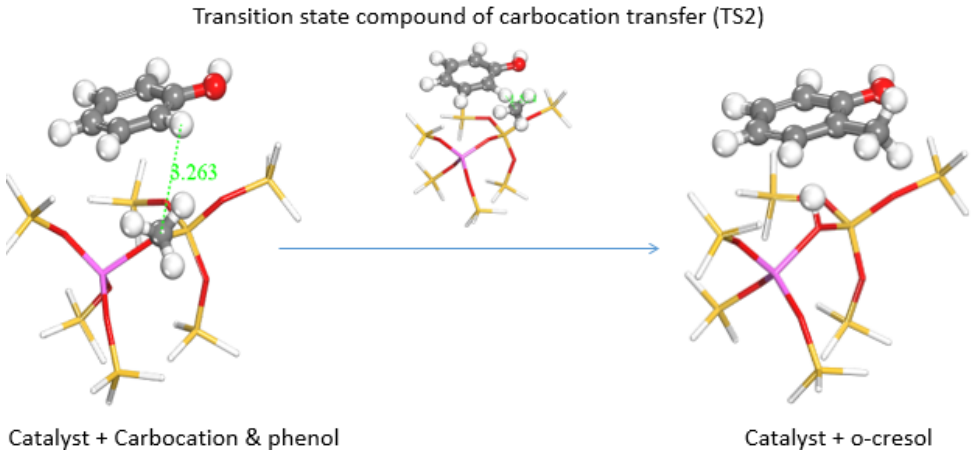


(b)

*Fig 2. (a) CSP3-O bond (C8-O7) cleavage and carbocation formation; (b) Methyl carbocation transfer to ortho-position of phenol (transfers to meta- and para-positions are not shown here). Atoms are colored as follows: carbon atom (grey), hydrogen atom (light grey), oxygen atom (red), silica atom (yellow) and aluminum atom (pink).*

The model also predicted that the energy barrier for the methyl cleavage in the presence of the catalyst was 66.4 kcal/mol, which is much lower than the energy barrier values of the non-catalytic process. Moreover, compared to the non-catalytic process, the energy barrier for catalytic transmethylation to ortho-position decreased from 105.5 kcal/mol to 60.7 kcal/mol, and those for para- and meta-positions dropped from 107.3 kcal/mol to 66.1 kcal/mol and from 118.0 kcal/mol to 67.2 kcal/mol respectively. These results are also in line with experimental data which showed that a lower temperature (approximately by 150˚C) was required to achieve a similar conversion ratio during the catalytic decomposition of anisole compared to non-catalytic decomposition [42].

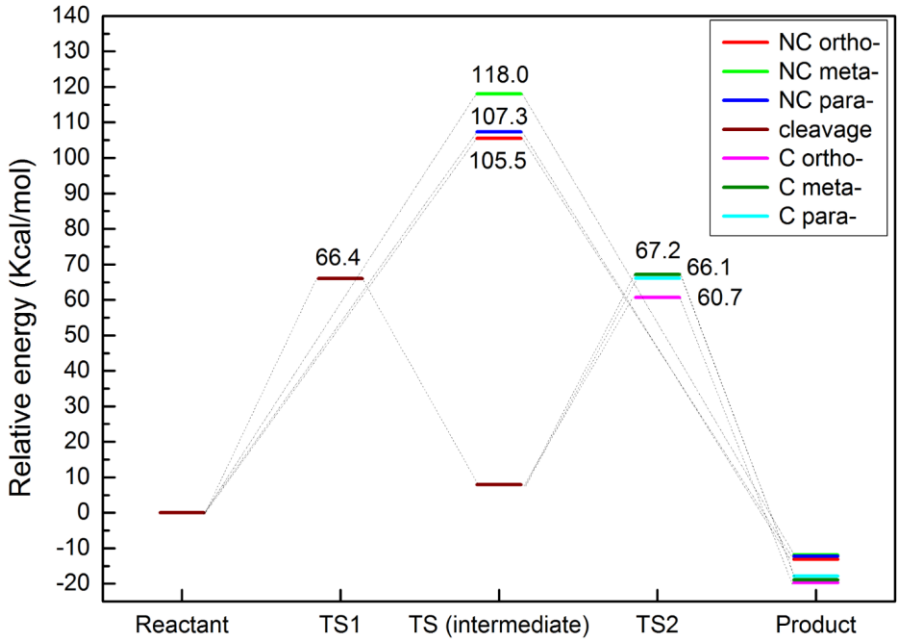


*Fig 3. Energy barriers for transmethylation reactions of anisole to cresol (via phenol). (C denotes to catalytic transmethylation; NC denotes to non-catalytic transmethylation)*

### 3.3 Modelling of non-catalytic and catalytic transmethylation of anisole to other acceptor molecules

Besides the cresol, the transmethylation process also gives rise to other methyl substituted compounds [42]. Therefore, transmethylation reactions with other acceptor molecules were modelled to assess the reactivity of these intermediate compounds, and the selectivity of the resulting products. The formation of toluene, methyl anisole, xylene, xylenol, and trimethyl-phenol due to the addition of a methyl group to benzene, anisole, toluene, cresol and xylenol respectively were also modelled. The energy barriers for the different reactions pathways in non-catalytic and catalytic decomposition of anisole are shown in Table 1.

In the case of non-catalytic decomposition, the energy barriers of transmethylation changed significantly, depending on the acceptor molecules. This is related to the fact that the substituents on the molecule affect the electron distribution in the aromatic ring, giving rise to the site migration of substituted reactions [47]. Anisole, toluene and phenolic compounds showed energy barrier values between 105.7 and 121.1 kcal/mol in the non-catalytic transmethylation (Table 1), and the energy barrier for the methyl transfer to benzene in the non-catalytic reaction was the highest for 126.4 kcal/mol.

It is found the molecules containing branch chain substituents, especially oxygen-rich chains such as hydroxy and methoxy functional groups, are more readily to accept methyl radicals.

The branch chains may have impact on the π-bond of the benzene ring, making the ring more susceptible to methyl attack especially at the ortho- and para-positions, while the benzene ring without branch chains may have smaller electron density, so that is more stable to radical attack [48].

It was observed that transmethylation to phenol and o-cresol exhibited intrinsic preference in the ortho- and para-positions, which is in line with the results from the Fukui analyses for electrophilic attack to phenol molecule (Fig S3(b)). On the other hand, toluene and anisole showed moderate difference (within 4.1 kcal/mol) in position preference for non-catalytic transmethylation. This is because the free pair of electrons in the oxygen of the hydroxyl group are more likely to move to the ring, and consequently affect the ring property; while less electron migration and less impact onto the ring occurs with the methyl group attached either directly to the ring (in the case of toluene) or to the oxygen (in the case of anisole) [49].

*Table 1. Energy barrier for the different reaction pathways of transmethylation in non-catalytic and catalytic decomposition of anisole*

| Reactant | Via | Product | Orientation | Energy Barrier (kcal/mol) | | |
|---|---|---|---|---|---|---|
| | | | | Non-catalytic (TS) | Catalytic | |
| | | | | | Cleavage (TS1) | Methyl cation transfer (TS2) |
| Anisole | Phenol | Cresol | Ortho | 105.5 | 66.4 | 60.7 |
| | | | Meta | 118.0 | | 67.2 |
| | | | Para | 107.3 | | 66.1 |
| | o-Cresol | Xylenol | Ortho | 107.2 | | 60.4 |
| | | | Meta | 121.1 | | 61.8 |
| | | | Para | 107.0 | | 54.1 |
| | 2,4-Xylenol | 2,4,6-Phenol | Ortho | 114.3 | | 60.4 |
| | 2,6-Xylenol | 2,3,6-Phenol | Meta | 110.0 | | 59.9 |
| | Benzene | Toluene | - | 126.4 | | 73.5 |
| | Toluene | Xylene | Ortho | 108.1 | | 71.2 |
| | | | Meta | 112.2 | | 68.3 |

| | | | | | |
|---|---|---|---|---|---|
| | | | Para | 109.5 | 70.8 |
| | | | Ortho | 106.9 | 63.3 |
| | Anisole | Methyl-anisole | Meta | 105.7 | 67.0 |
| | | | Para | 108.3 | 71.7 |

In the case of catalytic reactions, the presence of the acid catalyst decreased notably the energy barrier values, exhibiting a big influence on promoting transmethylation. The decreases in the energy barrier was observed range from 36.6 kcal/mol (transmethylation to para position of anisole) to 59.3 kcal/mol (transmethylation to meta position of o-cresol). The transmethylation to benzene is found had the highest energy barrier for 73.5 kcal/mol, even though it has been diminished by roughly 53 kcal/mol compared to the non-catalytic process, this indicates the stability of the benzene ring to electrophilic attack compared to other branch chain contained compounds. In the case of the transmethylation to toluene, the model also predicted a decrease in the energy barrier value for each of the position transfers when using a catalyst (ranging between 68.3kcal/mol and 71.2kcal/mol), but the predicted energy barriers are higher than those for most oxygen contained compounds, regardless of the position transfer. It is also noted that transmethylation to anisole at the ortho-position to produce methyl-anisole exhibited a similar energy barrier value to other phenolic intermediate compounds (63.3 kcal/mol). This result suggests that the presence of sole methyl group attached to the aromatic ring has limited effect on the molecules to accept electrophilic substitution by methyl carbocation, this may attribute to the lower electronegativity of the methyl group than that of the oxygen contained functional groups [50]. In other words, hydroxyl and methoxyl groups are the most likely ones to promote the reactivity of the aromatic ring, followed by methyl group. Benzene molecule itself is the least reactive compound among the evaluated molecules in the catalytic transmethylation over the Brønsted acid sites. At a macroscopic level, it can be inferred that in the catalytic decomposition of anisole, majority of toluene and xylene are probably produced from the deoxygenation of cresols and xylenols, rather than from the transmethylation to benzene over the Brønsted acid sites.

Compared to AHs, methyl phenolic compounds, i.e. phenol, cresol and xylenol, are found to be prone to accept electrophilic substitution at all positions, even though a slight preference (values difference lower than 8 kcal/mol) for ortho- and para-positions were observed in the

case of phenol and cresol. Among all the evaluated compounds, these molecules accept methyl carbocation at the lowest energy barrier values. Transmethylation for cresol into xylenol presented energy barriers ranging from 54.1 kcal/mol (p-position transfer) to 61.8 kcal/mol (m-position transfer). Transmethylation to convert xylenol into 2,3,6-methyl phenol and 2,4,6-methyl phenol exhibited similar energy barriers at around 60 kcal/mol. These results well illustrate the experimental results during catalytic decomposition of anisole in which the abundant production of multi-methyl phenolic compounds and the typical position preference was observed [42]. The formation of these multi-methyl phenolic compounds from anisole depends on the initial formation of cresol.

## 4 CONCLUSION

This work presents the DFT modelling of the transmethylation as the primary reaction taking place in both non-catalytic and catalytic anisole decomposition. Methyl radical cleavage led to the transmethylation process in non-catalytic transmethylation, which primarily took place with the methyl free radical transfer. In catalytic transmethylation, reactants interacted with the Brønsted acid sites present in the catalyst. The catalytic transmethylation was initiated by the Brønsted acid proton electrophilic attack at the oxygen atom of anisole, followed by a carbocation substitution. A dual electrophilic attack mechanism was proposed for the catalytic transmethylation. Transmethylation reactions modelling, based on the proposed mechanism, proved that the Brønsted acid catalyst could significantly lower the reaction energy barrier for all reactant compounds investigated due to changes in the reaction pathways. Most of the energy barriers for the evaluated transmethylation reactions decreased more than 40 kcal/mol when considering the catalytic effect, the highest decrease being observed in the case of o-cresol (around 60 kcal/mol). Furthermore, both non-catalytic and catalytic transmethylation exhibited target molecule preference, depending on the original substituents of the acceptor, and transmethylation to most compounds showed preference for the ortho- and para-positions. Non-catalytic transmethylation to compounds with oxygen-rich substituents generally showed lower energy barriers. In the catalytic decomposition of anisole, the presence of oxygen-rich substituents also enhanced the reactivity of the ring, especially for phenolic compounds at the ortho- and para-positions. The lowest energy barrier was

observed in the case of transmethylation towards the para-position of the cresol molecule (54.1 kcal/mol).

## AUTHOR INFORMATION

### Corresponding Author

D.S.: 101011398@seu.edu.cn

### Author Contributions

All authors have given approval to the final version of the manuscript.

### Notes

The authors declare no competing financial interest.

## ACKNOWLEDGEMENT

The authors would like to acknowledge financial support from the National Natural Science Foundation of China (project references: 51476034 and 51628601), Natural Science Foundation of Jiangsu Province (project reference: BK20161423), and the FP7 Marie Curie iComFluid (project reference: 312261).

## REFERENCES

1 W. Boerjan, J. Ralph and M. Baucher, *Annu. Rev. Plant Biol.*, 2003, **54**, 519–546.

2 C. S. Lancefield and N. J. Westwood, *Green Chem.*, 2015, **17**, 4980–4990.

3 A. V. Bridgwater, *Biomass and Bioenergy*, 2012, **38**, 68–94.

4 A. V. Bridgwater and G. V. C. Peacocke, *Renew. Sustain. energy Rev.*, 2000, **4**, 1–73.

5 K. A. Jung, S. H. Woo, S.-R. Lim and J. M. Park, *Chem. Eng. J.*, 2015, **259**, 107–116.

6 L. Zhang, R. Liu, R. Yin and Y. Mei, *Renew. Sustain. Energy Rev.*, 2013, **24**, 66–72.

7 C. Liu, H. Wang, A. M. Karim, J. Sun, Y. Wang, M. Karim Ayman, J. Sun and Y. Wang, *Chem. Soc. Rev.*, 2014, **43**, 7594–7623.

8 S. Vichaphund, D. Aht-ong, V. Sricharoenchaikul and D. Atong, *Renew. Energy*, 2014, **65**, 70–77.

9 C. Mukarakate, J. D. McBrayer, T. J. Evans, S. Budhi, D. J. Robichaud, K. Iisa, J. ten

Dam, M. J. Watson, R. M. Baldwin and M. R. Nimlos, *Green Chem.*, 2015, **17**, 4217–4227.

10 C. Mukarakate, X. Zhang, A. R. Stanton, D. J. Robichaud, P. N. Ciesielski, K. Malhotra, B. S. Donohoe, E. Gjersing, R. J. Evans, D. S. Heroux, R. Richards, K. Iisa and M. R. Nimlos, *Green Chem.*, 2014, **16**, 1444.

11 G. Yildiz, M. Pronk, M. Djokic, K. M. Van Geem, F. Ronsse, R. Van Duren and W. Prins, *J. Anal. Appl. Pyrolysis*, 2013, **103**, 343–351.

12 D. K. Shen, S. Gu, K. H. Luo, S. R. Wang and M. X. Fang, *Bioresour. Technol.*, 2010, **101**, 6136–6146.

13 S. J. Hurff and M. T. Klein, *Ind. Eng. Chem. Fundam.*, 1983, **22**, 426–430.

14 Q. Meng, H. Fan, H. Liu, H. Zhou, Z. He, Z. Jiang, T. Wu and B. Han, *ChemCatChem*, 2015, **7**, 2831–2835.

15 T. Prasomsri, A. T. To, S. Crossley, W. E. Alvarez and D. E. Resasco, *Appl. Catal. B Environ.*, 2011, **106**, 204–211.

16 K. Wang, X. Dong, Z. Chen, Y. He, Y. Xu and Z. Liu, *Microporous Mesoporous Mater.*, 2014, **185**, 61–65.

17 J. Cornella, E. Gómez-Bengoa and R. Martin, *J. Am. Chem. Soc.*, 2013, **135**, 1997–2009.

18 C. Mackie, R. Doolan and F. Nelson, *J. Phys. Chem. C*, 1989, **93**, 664–670.

19 M. E. Sad, C. L. Padró and C. R. Apesteguía, *Catal. Today*, 2008, **133**–**135**, 720–728.

20 J. Xu, A. Z. Yan and Q. H. Xu, *Appl. Catal.*, 1999, **10**, 983–986.

21 W. Wang, P. L. De Cola, R. Glaeser, I. I. Ivanova, J. Weitkamp and M. Hunger, *Catal. Commun.*, 2004, **94**, 119–123.

22 M. Bregolato, V. Bolis, C. Busco, P. Ugliengo, S. Bordiga, F. Cavani, N. Ballarini, L. Maselli, S. Passeri and I. Rossetti, *J. Catal.*, 2007, **245**, 285–300.

23 K. G. Bhattacharyya, A. K. Talukdar, P. Das and S. Sivasanker, *J. Mol. Catal. A Chem.*, 2003, **197**, 255–262.

353 24 M. E. Sad, C. L. Padró and C. R. Apesteguía, *J. Mol. Catal. A Chem.*, 2010, **327**, 63–
354 72.

355 25 X. Zhu, R. G. Mallinson and D. E. Resasco, *Appl. Catal. A Gen.*, 2010, **379**, 172–181.

356 26 N. Ballarini, F. Cavani, L. Maselli, A. Montaletti, S. Passeri, D. Scagliarini, C. Flego
357 and C. Perego, *J. Catal.*, 2007, **251**, 423–436.

358 27 J. H. Baraban, P. B. Changala, G. C. Mellau, J. F. Stanton, A. J. Merer and R. W.
359 Field, *Science (80-. ).*, 2015, **350**, 1338–1342.

360 28 R. Thilakaratne, J.-P. Tessonnier and R. C. Brown, *Green Chem.*, 2016, **18**, 2231–
361 2239.

362 29 G. Li, L. Li, L. Shi, L. Jin, Z. Tang, H. Fan and H. Hu, *Energy & Fuels*, 2014, **28**, 980–
363 986.

364 30 Z. Geng, M. Zhang and Y. Yu, *Fuel*, 2012, **93**, 92–98.

365 31 Y. Huang, X. Dong, M. Li, Y. Yu, J. Gao, Y. Zheng, G. B. Fitzgerald, J. de Joannis, Y.
366 Tang, I. E. Wachs, S. G. Podkolzin, Y. Huang, X. Dong, M. Li, M. Zhang and Y. Yu,
367 *Catal. Sci. Technol.*, 2015, **5**, 1093–1105.

368 32 Y. Huang, X. Dong, M. Li, M. Zhang and Y. Yu, *RSC Adv.*, 2014, **4**, 14573.

369 33 J. Gao, Y. Zheng, G. B. Fitzgerald, J. de Joannis, Y. Tang, I. E. Wachs and S. G.
370 Podkolzin, *J. Phys. Chem. C*, 2014, **118**, 4670–4679.

371 34 Z. K. Li, Z. M. Zong, H. L. Yan, Y. G. Wang, X. Y. Wei, D.-L. Shi, Y. P. Zhao, C. L.
372 Zhao, Z. S. Yang and X. Fan, *Fuel*, 2014, **120**, 158–162.

373 35 B. Delley, *J. Chem. Phys.*, 1990, **92**, 508–517.

374 36 B. Delley, *J. Chem. Phys.*, 2000, **113**, 7756.

375 37 M. Elanany, M. Koyama, M. Kubo, P. Selvam and A. Miyamoto, *Microporous*
376 *mesoporous Mater.*, 2004, **71**, 51–56.

377 38 B. Kalita and R. C. Deka, *Eur. Phys. J. D*, 2009, **53**, 51–58.

378 39 J. P. Perdew, K. Burke and M. Ernzerhof, *Phys. Rev. Lett.*, 1996, **77**, 3865–3868.

379 40 S. Grimme, *J. Comput. Chem.*, 2006, **27**, 1787–1799.

380 41 F. L. Hirshfeld, *Theor. Chim. Acta*, 1977, **44**, 129–138.

381 42 J. Zhang, B. Fidalgo, D. Shen, R. Xiao and S. Gu, *J. Anal. Appl. Pyrolysis*, 2016, **122**,
382 323–331.

383 43 J. F. Haw, B. R. Richardson, I. S. Oshiro, N. D. Lazo and J. a. Speed, *J. Am. Chem.*
384 *Soc.*, 1989, **111**, 2052–2058.

385 44 B. R. Richardson, N. D. Lazo, P. D. Schettler, J. L. White and J. F. Haw, *J. Am. Chem.*
386 *Soc.*, 1990, **112**, 2886–2891.

387 45 E. J. Munson, T. Xu and J. F. Haw, *J. Chem. Soc. Chem. Commun.*, 1993, 75–76.

388 46 E. J. M. and J. F. H. Teng Xu, Jinhua Zhang, *Chem. Commun.*, 1994, 2733–2735.

389 47 F. L. Lambert, *J. Chem. Educ.*, 1958, **35**, 342–343.

390 48 T. Phuong, *J. Catal.*, 1986, **102**, 456–459.

391 49 X. Zhu, L. L. Lobban, R. G. Mallinson and D. E. Resasco, *J. Catal.*, 2011, **281**, 21–29.

392 50 F. De Proft, W. Langenaeker and P. Geerlings, *J. Phys. Chem.*, 1993, **97**, 1826–1831.

# Supplementary Information

Table S1: Unique imaginary frequency identified for each transition state of the reactions for both non-catalytic and catalytic transmethylation

| Reactant | Via | Product | Orientation | Imaginary frequency (Frequency(1/cm); Intensity(km/mol)) | | |
|---|---|---|---|---|---|---|
| | | | | Non-catalytic (TS) | Catalytic | |
| | | | | | Cleavage (TS1) | Methyl cation transfer (TS2) |
| anisole | phenol | Cresol | Ortho | -15.49/0.03 | -331.54/99.74 | -352.36/6.86 |
| | | | Meta | -11.96/0.14 | | -285.63/7.12 |
| | | | Para | -10.15/0.11 | | -435.58/5.90 |
| | o-cresol | Xylenol | Ortho | -304.25/658.68 | | -345.63/7.72 |
| | | | Meta | -144.6/1.40 | | -311.78/158.17 |
| | | | Para | -270.32/163.89 | | -343.56/192.81 |
| | 2,4-xylenol | 2,4,6-phenol | Ortho | -237.38/453.09 | | -171.58/6.64 |
| | 2,6-xylenol | 2,3,6-phenol | Meta | -229.42/129.61 | | -511.45/499.08 |
| | benzene | Toluene | - | -686.39/37.85 | | -233.06/16.67 |
| | toluene | Xylene | Ortho | -244.71/129.42 | | -138.44/101.67 |
| | | | Meta | -240.01/87.44 | | -320.08/188.36 |
| | | | Para | -36.49/27.64 | | -302.45/185.02 |
| | anisole | methyl-anisole | Ortho | -283.22/185.03 | | -98.98/4.73 |
| | | | Meta | -6823.26/7.10 | | -313.60/67.33 |
| | | | Para | -267.68/159.39 | | -309.34/2.79 |

Fig S2. (a) Mulliken bond order of the anisole molecule for the transmethylation reaction; (b) Fukui indices of anisole atoms under electrophilic attack (Fukui (-)). Isovalue 0.035. Atoms are colored as follows: carbon atom (grey), hydrogen atom (white) and oxygen atom (red)

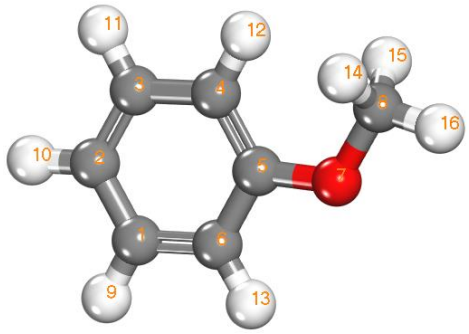


| Bond ID | Mulliken Bond order |
|---|---|
| C8-O7 | 0.515 |
| C5-O7 | 0.668 |
| C8-H14 | 0.798 |
| C8-H15 | 0.799 |
| C6-H13 | 0.813 |
| C4-H12 | 0.814 |
| C3-H11 | 0.821 |
| C1-H9 | 0.824 |
| C2-H10 | 0.825 |
| C8-H16 | 0.826 |
| C4-C5 | 1.003 |
| C3-C4 | 1.025 |
| C5-C6 | 1.030 |
| C1-C2 | 1.032 |
| C1-C6 | 1.054 |
| C2-C3 | 1.063 |

*(a)*

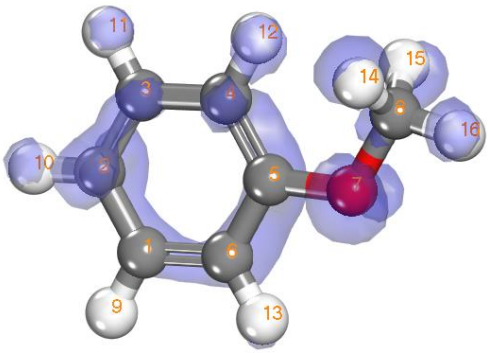


| Atom | Fukui (-) index |
|---|---|
| O7 | 0.129 |
| C2 | 0.125 |
| C6 | 0.086 |
| C5 | 0.075 |
| C4 | 0.072 |
| C3 | 0.071 |
| C1 | 0.061 |
| H10 | 0.057 |
| H11 | 0.046 |
| H13 | 0.046 |
| H9 | 0.044 |
| H12 | 0.040 |
| H15 | 0.038 |
| H14 | 0.037 |
| H16 | 0.036 |
| C8 | 0.035 |

*(b)*

Fig S3. Fukui indices for (a) radical attack on phenol molecule (Fukui (0)), and (b) electrophilic attack on phenol molecule (Fukui (-)). Isovalue 0.035. Atoms are colored as follows: carbon atom (grey), and hydrogen atom (white) and oxygen atom (red)

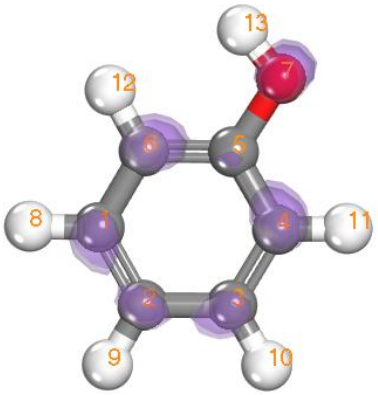


| Atom | Fukui (0) index |
|---|---|
| C4 | 0.105 |
| O7 | 0.103 |
| C2 | 0.102 |
| C6 | 0.100 |
| C1 | 0.099 |
| C3 | 0.095 |
| C5 | 0.073 |
| H8 | 0.057 |
| H10 | 0.056 |
| H11 | 0.056 |
| H9 | 0.055 |
| H12 | 0.055 |
| H13 | 0.044 |

*(a)*

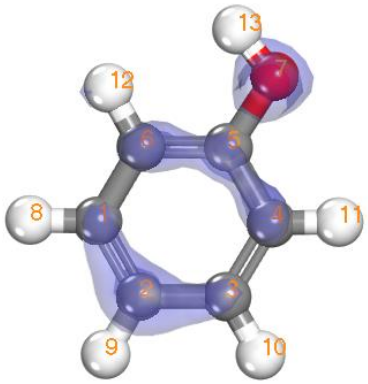


| Atom | Fukui (-) index |
|---|---|
| O7 | 0.152 |
| C2 | 0.136 |
| C4 | 0.089 |
| C5 | 0.089 |
| C6 | 0.083 |
| C1 | 0.073 |
| C3 | 0.068 |
| H9 | 0.061 |
| H13 | 0.055 |
| H11 | 0.050 |
| H8 | 0.049 |
| H10 | 0.048 |
| H12 | 0.048 |

*(b)*

https://dspace.org/

# Mechanism of transmethylation in anisole decompostion over Brønsted acid sites: Density Functional Theory (DFT) study

**Zhang, Jiajun; Fidalgo, Beatriz; Kolios, Athanasios; Shen, Dekui; Gu, Sai**

**2017-08-15**
Royal Society of Chemistry
http://dx.doi.org/10.1039/C7SE00280G
Zhang J, Fidalgo B, Kolios A, Shen D, Gu S, Mechanism of transmethylation in anisole decomposition over Brønsted acid sites: Density Functional Theory (DFT) study, Sustainable Energy & Fuels, Vol. 1, Issue 8, 2017, pp. 1788-1794

Downloaded from a DSpace repository. https://dspace.org/